Utah State University

DigitalCommons@USU

Space Dynamics Lab Publications

Space Dynamics Lab

Measurement of the Nitric Oxide Altitude Distribution in the Mid-Latitude Mesosphere

K. D. Baker

A. F. Nagy

R. O. Olsen

E. S. Oran

J. Randhawa

D. F. Strobel
Utah State University

See next page for additional authors

Follow this and additional works at: https://digitalcommons.usu.edu/sdl_pubs

Recommended Citation

Utah State University
MERRILL-CAZIER LIBRARY

Authors

K. D. Baker, A. F. Nagy, R. O. Olsen, E. S. Oran, J. Randhawa, D. F. Strobel, and T. Tohmatsu

Baker, K. D., A. F. Nagy, R. O. Olsen, E. S. Oran, J. Randhawa, D. F. Strobel, and T. Tohmatsu. 1977. "Measurement of the Nitric Oxide Altitude Distribution in the Mid-latitude Mesosphere." *Journal of Geophysical Research* 82 (22): 3281–86. doi:10.1029/JA082i022p03281.

MEASUREMENT OF THE NITRIC OXIDE ALTITUDE DISTRIBUTION IN THE MID-LATITUDE MESOSPHERE

K. D. Baker[1], A. F. Nagy[1,2], R. O. Olsen[3], E. S. Oran[4],
J. Randhawa[3], D. F. Strobel[4], and T. Tohmatsu[5]

Abstract. A simple rocket-borne system has been developed for deriving nitric oxide concentration in the mesosphere from measurements of resonantly scattered solar ultraviolet radiation in the NO gamma band near 2150 Å. The NO signal is extracted from a background of Rayleigh-scattered light by a direct measurement of this scattered light by use of an NO absorption cell. This system was utilized to measure the NO concentration above White Sands, New Mexico, in the altitude range from 69 to 101 km. The derived NO profile shows a concentration of about 3×10^7 cm^{-3} at 67 and 100 km with a deep valley (more than an order of magnitude less) at about 84 km. Comparison with model calculations indicates that the time constant for NO chemistry is smaller than or comparable with that for transport.

Introduction

Satellite and rocket measurements of nitric oxide gamma band fluorescence can be used to deduce nitric oxide concentrations in the thermosphere and mesosphere [Barth, 1964, 1966a, b]. In the mesosphere the measurement is complicated by a background signal due to Rayleigh scattering of solar radiation by atmospheric molecules. The satellite-borne spectrometers provide meaningful data only about 90 km, where Rayleigh scattering is small [Rusch, 1973; Barth et al., 1973; Rusch and Barth, 1975].

A number of vertical NO density profiles in the 70- to 110-km region have been inferred from rocket-borne spectrometer measurements of γ (1, 0) band fluorescence [e.g., Barth, 1966a, b; Pearce, 1969; Meira, 1971; Tisone, 1973]. In the mesosphere the subtraction of a large Rayleigh scattering component from the measured signal is necessary to recover the small γ (1, 0) band column emission rate. Since the Rayleigh scattering component is normally deduced from atmospheric density measurements, the resultant γ (1, 0) band column emission has large uncertainties associated with it. To deduce the volume emission rate and hence the local NO density, differentiation of the noisy column emission is required; and therefore the error bars are large on the derived NO concentrations below the mesopause.

A small and uncomplicated photometer system has been developed for rocket-borne NO measurements which allows us, in principle, to obtain accurately both the γ (1, 0) band emission and the background Rayleigh-scattered component [Tohmatsu and Iwagami, 1975]. The purpose of this brief note is to describe this photometer system and to present a rocket measurement of the NO concentration about White Sands, New Mexico, on October 4, 1973. The measurement is compared with previous fluorescence measurements of NO with theoretical calculations.

Instrument Description

The rocket experiment uses an ultraviolet photometer coupled with a nitric oxide gas-filled optical absorption cell to remove correctly the Rayleigh-scattered background signal and to measure accurately the small γ (1, 0) band emission in the mesosphere. The block diagram (Figure 1) illustrates the basic principle of operation of the photometer system. An 18-cm solar baffle 6.4 cm in diameter and a honeycomb collimator with a circular field of view of 6° precede an interference filter. The center wavelength of this prefilter is 2160 Å with a half-power transmission width of 80 Å. Two optical cells are alternately placed into the optical path between the prefilter and the photomultiplier tube (Hammamatsu R431S). The optical cells are 3 cm in diameter, have a 2-cm path length, and are made of optical silica. The first cell is unfilled, while the second is filled with pure NO at a pressure of 200 torrs. These cells are cycled back and forth at a frequency of 1 Hz. The NO cell acts as a rejection filter for NO gamma band emissions terminating at the ground vibrational level (v" = 0). Figure 2 reproduces the results of a laboratory test showing clearly the removal of the (0, 0), (1, 0), and (2, 0) bands by the NO cell, while the other features (v" ≠ 0) remain unchanged. Thus the difference in the output signal with the different cells in the optical path corresponds to the intensity of the (1, 0) gamma band of NO at 2148 Å. A discussion of the calibration and data analysis details are given by Tsang [1975] and Tohmatsu and Iwagami [1976].

Results

The NO photometer system described above was flown aboard a Nike-Apache rocket launched from the White Sands Proving Grounds at 1854 MDT on October 4, 1973. The solar zenith angle was 92.15° at launch and 92.7° at the time of rocket apogee. The nose tip cover was ejected at an altitude of 69 km, and the rocket reached an apogee of 101 km; useful data were obtained only during the upleg portion of the flight. The photometer sampling rate was 18 samples/s, and the zenith

[1]Center for Research in Aeronomy, Utah State University, Logan, Utah   84322.
[2]Department of Atmospheric and Oceanic Sciences, University of Michigan, Ann Arbor, Michigan   48109.
[3]Atmospheric Science Laboratory, White Sands Missile Range, New Mexico   88002.
[4]Naval Research Laboratory, Washington, D. C.   20375.
[5]Geophysics Research Laboratory, University of Tokyo, Tokyo 113, Japan.
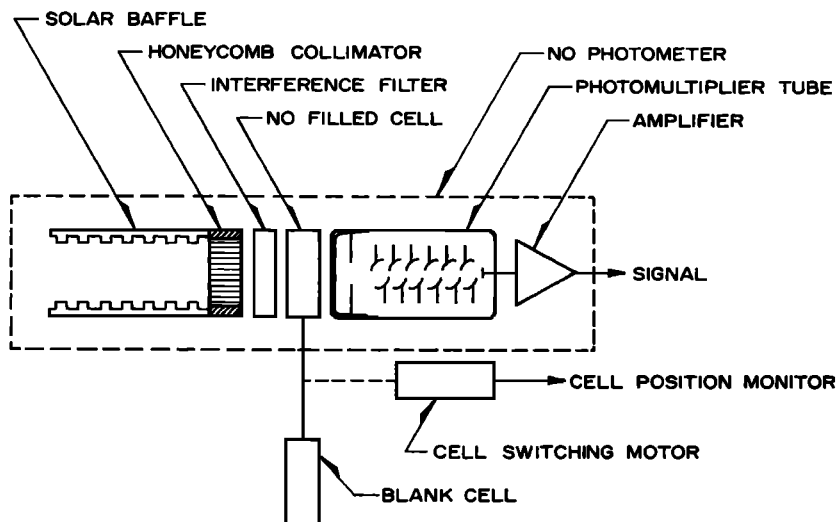
Fig. 1. Schematic of photometer system for measurement of nitric oxide gamma band fluorescence.

intensities (raw data points corrected for rocket aspect) thus obtained are shown in Figure 3. These data points were averaged over the period of cell dwell position ($\sim$0.5 s) and the signal with the NO cell in position subtracted from the signal with the blank cell in position. The resulting (1, 0) gamma band zenith emission data are shown in Figure 4. A polynomial least squares fit to these data points and plus or minus one

standard deviation flags is also shown in Figure 4. The resulting polynomial expression was differentiated to yield the volume emission rate and then converted to the NO densities shown in Figure 5 with an emission rate factor g of 7.68×10^{-6} [Cravens, 1977]. A check for the possible extinction of solar radiation at 2150 Å by ozone (ozone densities were taken from the U.S. Standard Atmosphere (1976) and the absorption cross section
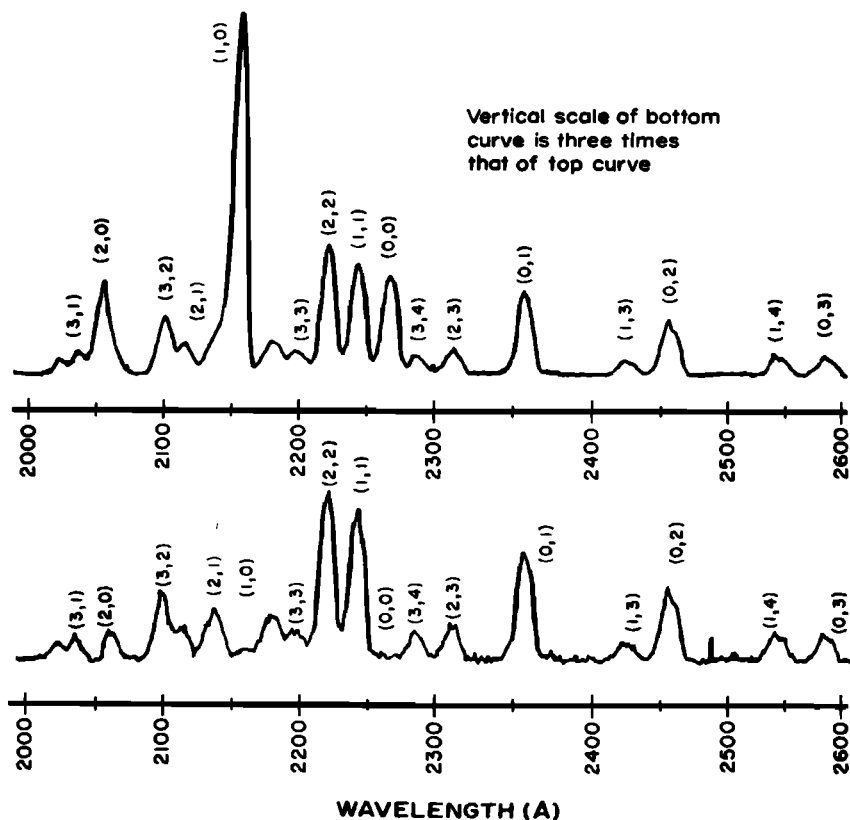

WAVELENGTH (A)

Fig. 2. Laboratory spectra of NO gamma band fluorescence. (Top) Spectrum taken with blank cell. (Bottom) Spectrum taken with NO absorption cell. Note that the v" = 0 progression bands are completely removed in the lower spectrum.

from Hudson and Kieffer [1975] indicated that the
ozone optical depth $\tau_{O_3}(2150$ Å) was less than 0.1,
even as low as 70 km. It was also established
that the sunward column density of NO was less
than 1.5×10^{15}, which according to the work of
Cravens [1977] would reduce the emission rate
factor by less than 10%. Considering the present
uncertainties ($\sim$10%) in this rate, it was con-
sidered inappropriate to attempt to introduce any
corrections. Figure 5 also shows, for the sake
of comparison, other inferred mid-latitude NO
density profiles (normalized by using the pres-
ently accepted value of the g factor).

Model Calculations and Discussion

One complication in modeling the experimental
results is that October 3, 1973, was a geomag-
netically disturbed day. Analysis of Atmosphere
Explorer (AE) data has shown that geomagnetic
storms produce large-scale horizontal gravity
waves that propagate away from the auroral zones
as well as a meridional circulation that trans-
ports NO-rich air from the auroral regions to
mid-latitudes [Cravens and Stewart, 1976]. As
the temperature perturbations propagate through
the atmosphere, they locally enhance the reac-
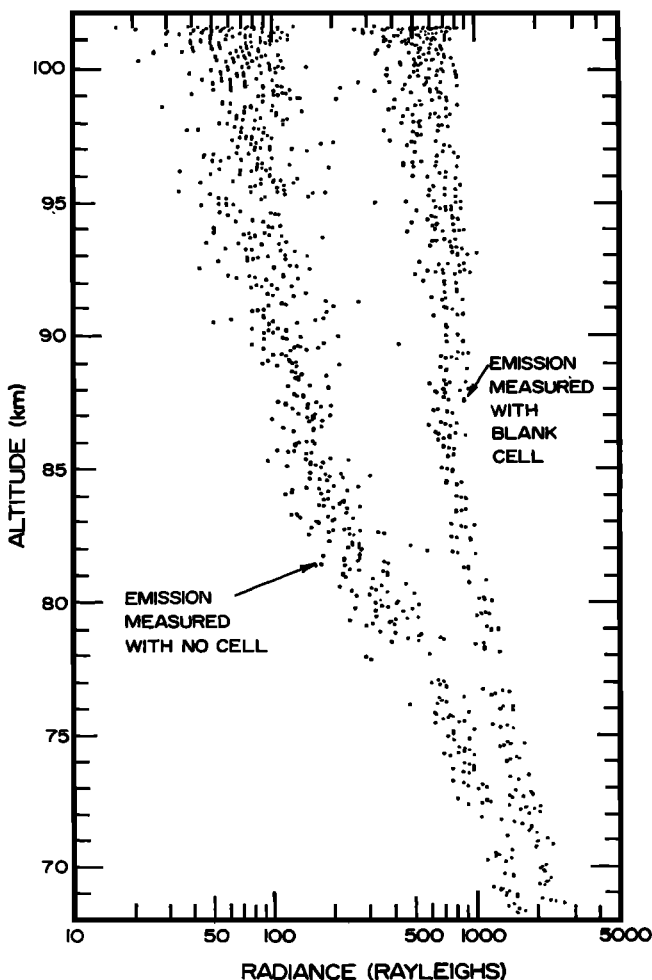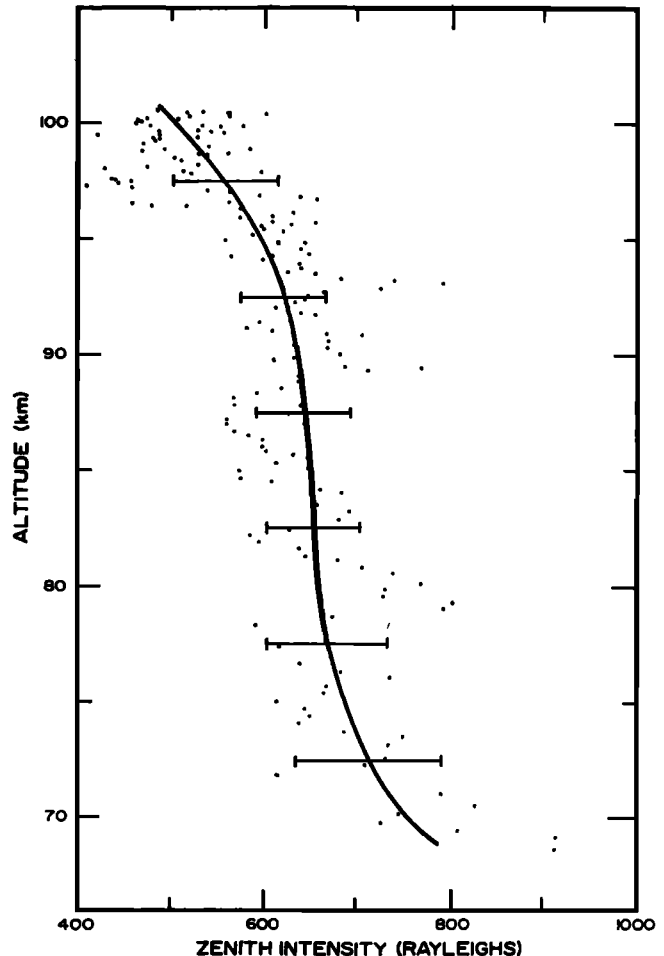tion rates of $N(^4S) + O_2 \rightarrow NO + O$ and cause sub-

Fig. 4. The zenith emission of the NO (1, 0)
gamma band measured with rocket-borne photometer.

stantial amounts of $N(^4S)$ to be converted to NO.
To include all these physical processes in a
model is beyond the scope of this brief report.
Instead, we used the Naval Research Laboratory
model of atmospheric odd nitrogen which is part
of a one-dimensional model of the mid-latitude
ionosphere [Oran et al., 1975; Strobel et al.,
1976]. The primary region of interest is below
95 km, where the production rate of odd nitrogen
is exceedingly small. The major NO source is a
downward flux from the thermosphere that can be
simulated if the observed NO concentration at
100 km can be approximately calculated. Such a
procedure has been successfully employed by
Strobel [1971, 1972]. One uncertain parameter
in odd nitrogen models is the reaction rate of
$N(^2D) + O \rightarrow N(^4S) + O$. Davenport et al. [1976]
have measured a rate of 1.7×10^{-12} cm^3 s^{-1} at
300°K in the laboratory, whereas Frederick and
Rusch [1977] have inferred 4×10^{-13} cm^3 s^{-1} at
thermospheric temperatures from Atmosphere Ex-
plorer data analysis. To obtain the observed NO
concentration at 100 km, we used the reaction
rate inferred by Frederick and Rusch [1977].

In Figure 6 the results of our model calcula-
tions are shown for three choices of eddy dif-
fusion coefficient profiles: (1) K = 4.5×10^6,
(2) K = 1×10^6, and (3) K = 1×10^6 exp
$[(z - 100$ km$)/2H]$ cm^2 s^{-1}. Case 3 obviously
gives the best fit to the observational data.

Fig. 3. Raw data points of zenith intensities
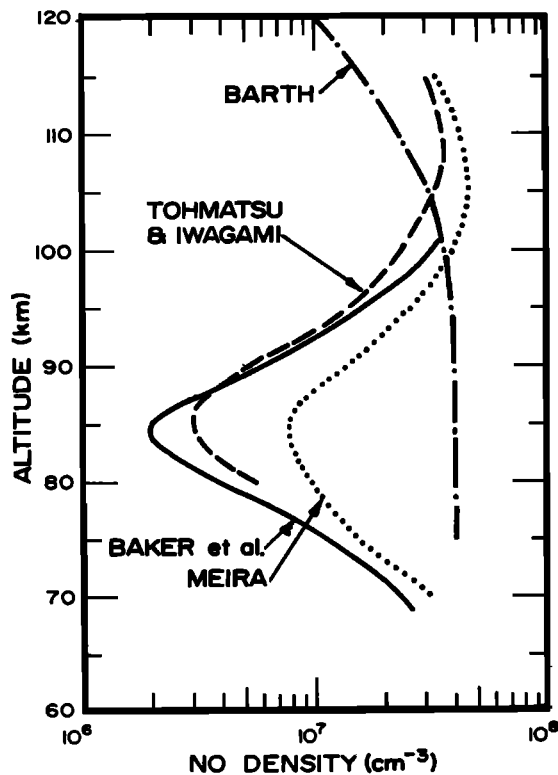observed with the NO cell and the blank cell.

Fig. 5. Nitric oxide density profile deduced from the data of Figure 4 compared with profiles of other workers [Barth, 1966b; Meira, 1971; Tohmatsu and Iwagami, 1975].

To understand the basic chemistry and physics that determine the NO density profile below 100 km, it is instructive to consider analytic solutions to the relevant NO flux and continuity equations

$$\phi = -K\left[\frac{dn}{dz} + \left(\frac{1}{T}\frac{dT}{dz} + \frac{1}{H}\right)n\right] \qquad (1a)$$

$$d\phi/dz = -J^*n \qquad (1b)$$

respectively, where H is the scale height of the background atmosphere, J^* is twice the diurnally averaged predissociation rate of NO and reflects the fact that the N atom produced in dissociation reacts and removes another NO molecule, and the other symbols have their customary meanings. If we assume that J^*, K, and T have constant values throughout this region, then we obtain

$$n = c_1 \exp[p_+(z - 95)] + c_2 \exp[p_-(z - 95)] \qquad (2)$$

where

$$p_\pm = -\frac{1}{2H}\left[1 + (1 + r)^{\frac{1}{2}}\right] \qquad r = 4H^2J^*/K > 0 \qquad (3)$$

and z is in kilometers. The appropriate boundary conditions are $n \simeq 1.3 \times 10^7$ cm^{-3} at 95 km (cf. Figure 6) and $\phi \simeq 0$ at 70 km as discussed in Oran et al. [1975]. (Note that the numerical accuracy of the computer solution for n is not sufficient to enforce $\phi = 0$ at 70 km. In practice, the solution satisfies $|\phi| < 10^7$ cm^{-2} s^{-1} at 70 km.)

For case 1 with H = 5.8 km, $J^* = 3.8 \times 10^{-6}$ s^{-1}, and K = 4.5×10^6 cm^2 s^{-1} we find r $\simeq$ 2 and the asymptotic (r $\to$ 0) solution approximates

$$p_+ \simeq 0$$
$$p_- \simeq -1/H \qquad (4)$$

Here the p_+ term represents the maximum diffusion velocity solution, while the p_- term represents a mixed distribution and zero velocity, as was previously discussed by Strobel [1971]. For the 70- to 100-km region the p_+ term is appropriate and the NO density is essentially constant throughout this region, since diffusion occurs more rapidly than chemistry.

For case 2 we find

$$r \simeq 10$$
$$p_+ \simeq 0.2 \text{ km}^{-1} \qquad (5)$$
$$p_- \simeq -0.4 \text{ km}^{-1}$$

Hence we expect in the 85- to 95-km region that the NO density will decrease with decreasing altitude as exp [0.2(z - 95 km)], whereas below 85 km we anticipate a rapid increase in the NO density with decreasing altitude as exp [-0.4(z - 95 km)]. From the definition of r we deduce that r $\simeq$ 10 implies comparable time constants for diffusion and dissociation. Case 2 corresponds to the downward NO flux from the thermosphere being
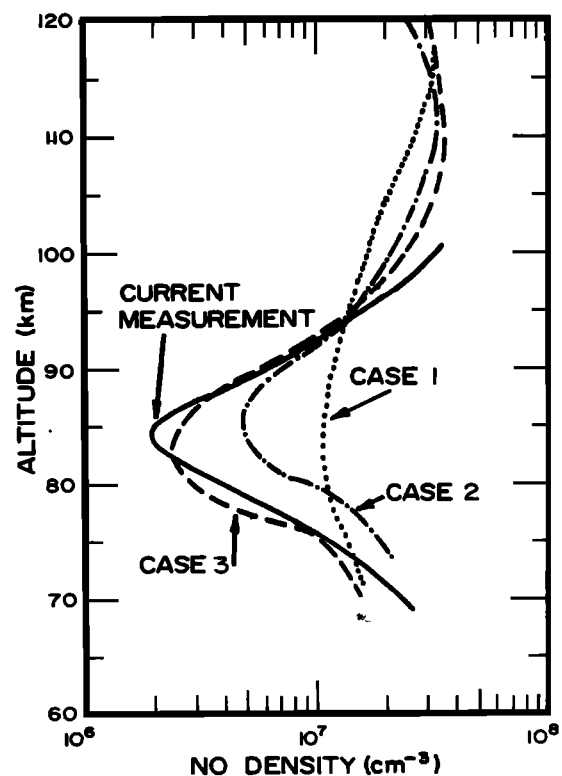

Fig. 6. Comparison of currently reported rocket measurement of NO density with three model calculations using different eddy diffusion coefficients: case 1, 4.3×10^6; case 2, 1×10^6; and case 3, $1 \times 10^6 \exp[(z - 100 \text{ km})/2\text{H}]$ cm^2 s^{-1}.

chemically depleted by predissociation in the δ
bands and the subsequent reaction of the product
N atoms to form N_2. When most of the NO molecules
have been chemically removed (by approximately
85 km), the NO density profile assumes a quasi-
mixed distribution with the departures due to
predissociation. In addition, there is a small
upward flux of NO molecules from the upper strat-
osphere to this chemical sink in the upper meso-
sphere [McConnell and McElroy, 1973; Brasseur and
Nicolet, 1973]. The magnitude of this flux is
sufficiently small to maintain a quasi-mixed den-
sity profile.

Case 3 ($r \simeq$ 40-60) represents the opposite ex-
treme where $r \rightarrow \infty$ and

$$P_+ \simeq +(J/K)^{\frac{1}{2}}$$
$$P_- \simeq -(J/K)^{\frac{1}{2}}$$
(6)

Here chemistry is more rapid than diffusion, and
a very deep minimum in the NO concentration pro-
file can be formed with characteristic density
height scales of $(K/J)^{\frac{1}{2}}$ above and below the mini-
mum.

The vertical NO density profiles that have
been inferred from NO fluorescence in γ (1, 0)
and that are shown in Figure 5 suggest that the
value of r is in excess of about 10. This would
imply that the time constant for NO chemistry is
comparable to or smaller than the transport time
constant. It should be realized that large er-
ror bars are associated with local NO densities
and that the conclusions are not definitive. An
alternate interpretation is that the structure in
the NO profile is due to large variations in the
eddy diffusion coefficient [Donahue, 1972; Rusch,
1973]. However, the eddy diffusion coefficient
in all odd nitrogen models is used as a lumped-
transport parameter representing all scales of
motion, and it is highly unlikely that its mag-
nitude changes by an order of magnitude in s
scale height.

Summary

The results presented here indicate that a
simple and inexpensive photometer system can be
used to determine the altitude distribution of
nitric oxide in the mesosphere. The inferred NO
density profile is in reasonably good agreement
with the earlier results obtained by Meira [1971]
and Tohmatsu and Iwagami [1975]. Since our γ
(1, 0) band fluorescence measurements were made
the day after a geomagnetic storm, the observed
NO concentrations could not be predicted with a
one-dimensional model of the thermosphere. How-
ever, we were able to describe the essential
chemistry and physics that control the vertical
NO density profile in the 70- to 100-km region in
terms of an analytic solution and the nondimen-
sional parameter r = $4H^2J^*/K$. The experimental
results presented here, as well as those of Meira
[1971] and Tohmatsu and Iwagami [1975], are con-
sistent with r $\gtrsim$ 10. We infer from this that
the NO time constant for chemistry is smaller
than or comparable to the transport time constant
in the mesosphere.

References

Barth, C. A., Rocket measurement of the nitric
oxide dayglow, J. Geophys. Res., 69, 3301, 1964.
Barth, C. A., Nitric oxide in the upper atmo-
sphere, Ann. Geophys., 22, 198, 1966a.
Barth, C. A., Rocket measurement of nitric oxide
in the upper atmosphere, Planet. Space Sci., 14,
623, 1966b.
Barth, C. A., D. W. Rusch, and A. I. Stewart, The
UV nitric oxide experiment on Atmosphere Ex-
plorer, Radio Sci., 8, 379, 1973.
Brasseur, G., and M. Nicolet, Chemospheric pro-
cesses of nitric oxide in the mesosphere and
stratosphere, Planet. Space Sci., 21, 939, 1973.
Cravens, T. E., Nitric oxide gamma band emission
rate factor, Planet. Space Sci., in press, 1977.
Cravens, T. E., and A. I. Stewart, The global
morphology of nitric oxide (abstract), EOS
Trans. AGU, 57, 295, 1976.
Davenport, J. E., T. G. Slanger, and G. Black,
The quenching of $N(^2D)$ by $O(^3P)$, J. Geophys.
Res., 81, 12, 1976.
Donahue, T. M., Positive ion chemistry of the D
and E regions, Radio Sci., 7, 73, 1972.
Frederick, J., and D. W. Rusch, On the chemistry
of metastable atomic nitrogen in the F region
deduced from simultaneous satellite measure-
ments of the 5200-Å airglow and atmospheric
composition, J. Geophys. Res., in press, 1977.
Hudson, R. D., and L. I. Kieffer, Absorption cross
sections of stratospheric molecules, CIAP monogr.
1, DOT-TST-75-71, Dep. of Transp., Washington,
D. C., 1975.
McDonnell, J. C. and M. B. McElroy, Odd nitrogen
in the atmosphere, J. Atmos. Sci., 30, 1465,
1973.
Meira, L. G., Jr., Rocket measurements of upper
atmospheric nitric oxide and their consequences
to the lower ionosphere, J. Geophys. Res., 76,
202, 1971.
Oran, E. S., P. S. Julienne, and D. F. Strobel,
The aeronomy at odd nitrogen in the thermosphere,
J. Geophys. Res., 80, 3068, 1975.
Pearce, J. B., Rocket measurement of nitric oxide
between 60 and 96 kilometers, J. Geophys. Res.,
74, 853, 1969.
Rusch, D. W., Satellite ultraviolet measurements
of nitric oxide fluorescence with a diffusive
transport model, J. Geophys. Res., 78, 5676,
1973.
Rusch, D. W., and C. A. Barth, Satellite measure-
ments of nitric oxide in the polar region, J.
Geophys. Res., 80, 3719, 1975.
Strobel, D. F., Odd nitrogen in the mesosphere,
J. Geophys. Res., 76, 8384, 1971.
Strobel, D. F., Nitric oxide in the D region, J.
Geophys. Res., 77, 1337, 1972.
Strobel, D. F., E. S. Oran, and P. D. Feldman,
The aeronomy of odd nitrogen in the thermosphere,
2, Twilight emissions, J. Geophys. Res., 81,
3745, 1976.

Tisone, G. C., Measurements of NO densities during
    sunrise at Kauai, J. Geophys. Res., 78, 746,
    1973.
Tohmatsu, T., and N. Iwagami, Measurement of ni-
    tric oxide distribution in the upper atmosphere,
    Space Res., XV, 241, 1975.
Tohmatsu, T., and N. Iwagami, Measurement of ni-
    tric oxide abundance in equatorial upper atmo-

sphere, J. Geomagn. Geoelec. Jap., 28, 343,
    1976.
Tsang, T. H., Analysis of results of a rocketborne
    photometer for measurements of nitric oxide,
    M.S. thesis, Utah State Univ., Logan, 1975.